Negative refraction of elastic waves in 2D phononic crystals : contribution of resonant transmissions to the construction of the image of a point source

Anne-Christine Hladky, Charles Croënne, Bertrand Dubus, Jerome O. Vasseur, L. Haumesser, D. Manga, B. Morvan

Negative refraction of elastic waves in 2D phononic crystals: Contribution of resonant transmissions to the construction of the image of a point source

Cite as: AIP Advances **1**, 041405 (2011); https://doi.org/10.1063/1.3676177
Submitted: 07 November 2011 • Accepted: 21 December 2011 • Published Online: 29 December 2011

Anne-Christine Hladky-Hennion, Charles Croënne, Bertrand Dubus, et al.

Negative refraction of elastic waves in 2D phononic crystals: Contribution of resonant transmissions to the construction of the image of a point source

Anne-Christine Hladky-Hennion,[1,a] Charles Croënne,[1] Bertrand Dubus,[1] Jérôme Vasseur,[1] Lionel Haumesser,[2] Dimitri Manga,[2,3] and Bruno Morvan[3]

[1]*Institut d'Électronique, de Microélectronique et de Nanotechnologie, UMR CNRS 8520, 41 Boulevard Vauban, 59046 Lille, France*
[2]*Laboratoire Imagerie et Cerveau, Université François Rabelais de Tours, ENIVL, 41034 Blois, France*
[3]*Laboratoire Ondes et Milieux Complexes, FRE-3102 CNRS, Place Robert Schuman, 76610 Le Havre, France*

(Received 7 November 2011; accepted 21 December 2011; published online 29 December 2011)

Negative refraction properties of a two-dimensional phononic crystal (PC), made of a triangular lattice of steel rods embedded in epoxy are investigated both experimentally and numerically. First, experiments have been carried out on a prism shaped PC immersed in water. Then, for focusing purposes, a flat lens is considered and the construction of the image of a point source is analyzed in details, when indices are matched between the PC and the surrounding fluid medium, whereas acoustic impedances are mismatched. Optimal conditions for focusing longitudinal elastic waves by such PC flat lens are then discussed. [doi:10.1063/1.3676177]

I. INTRODUCTION

Phononic crystals (PC's) may exhibit dispersion curves with a negative slope in the irreducible Brillouin zone i.e. the wave vector and the group velocity vector associated with an acoustic wave point in opposite directions. This property is typical of a left handed material and implies a negative index of refraction in the Snell-Descartes law. Negative refraction in phononic crystals has been the subject of numerous studies during the last fifteen years due to its potential application for focusing acoustic or elastic waves at the scale of the wavelength. Most of these studies were first devoted to phononic crystals with a fluid (liquid or air) matrix surrounding solid inclusions, in which only longitudinal waves propagate.[1–7] As demonstrated by J. Pendry for light in the frame of photonic crystals,[8] negative index phononic crystals may allow the realization of flat super-lenses able to focus acoustic waves with a resolution lower than the diffraction limit.[6] The super-resolution has been achieved for example using a PC lens made of a triangular array of steel cylinders immersed in methanol and surrounded with water.[7] Discussions of negative refraction phenomena in PC made of solid matrix are relatively few. In these systems, the co-existence of waves of different polarizations (longitudinal, transverse or shear waves) makes the analysis of negative refraction phenomena much more complex. Nevertheless, negative refraction of shear waves or of transverse waves was analyzed numerically in periodic arrays of holes drilled in a metal matrix.[9,10] More recently such phenomenon was reported for surface modes[11] or for plate modes[12,13] in solid matrix phononic crystals of finite thickness.

[a]Corresponding author : anne-christine.hladky@isen.fr

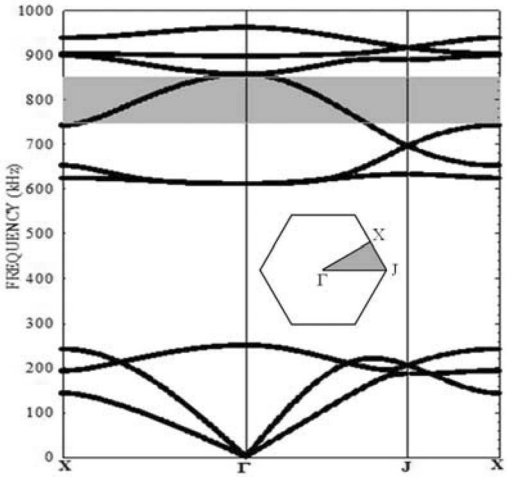

FIG. 1. Elastic band structure for the 2D PC made of a triangular array of steel rods in an epoxy matrix. The radius of the rods is 1 mm, the lattice parameter is 2.84 mm. In the frequency range [750 kHz, 860 kHz] (grey part) a negative branch is observed, corresponding to a mode with a predominantly longitudinal behaviour.

It is straightforward that superlenses based on solid matrix phononic crystals may have potential applications in the fields of medical imaging or ultrasonic beam-based therapy provided the negative refraction and then the focusing phenomenon involve longitudinal waves. Indeed it is necessary for this kind of applications, that the phononic crystal lens be surrounded by a fluid medium. In a recent paper, C. Croënne *et al.*[14] have shown theoretically and experimentally the negative refraction of a pure longitudinal elastic wave in a triangular array of steel rods inserted in an epoxy block. Preliminary analysis of the optimal conditions for elastic waves focusing in the surrounding fluid medium was also reported. The aim of the present paper is to analyze in more details the pressure field in the region where the focalization occurs in order to understand which parameters are of interest for the image construction. Therefore, section II presents the PC that exhibits negative refraction for longitudinal waves. In section III, experiments in water on a prism shaped PC exhibiting negative refraction are briefly reported. Then, a numerical study of the pressure field in the fluid surrounding medium is proposed in section IV, for a PC flat lens with a negative index, in order to highlight the focusing property of the lens. A comparison between a PC flat lens and a flat lens with effective properties (negative density and negative compressibility) is proposed in section V in order to understand how the formation of the image can be improved. Conclusions of this work are reported in section VI.

II. PRESENTATION OF THE PC

In this paper, the device of interest consists in a triangular array of steel rods embedded in epoxy. The diameter of the steel rods is 2 mm and the lattice parameter is 2.84 mm. For steel, the longitudinal wave velocity is 6180 m/s, the transverse wave velocity is 3245 m/s and the density is 7800 kg/m^3. For epoxy, the longitudinal wave velocity is 2440 m/s, the transverse wave velocity is 1130 m/s and the density is 1150 kg/m^3. The dispersion curves are calculated using the Finite Element Method and are presented on Fig. 1. It shows in the upper part a branch with a negative slope, in the frequency range [750 kHz, 860 kHz]. It corresponds to a mode with a predominantly longitudinal behavior. Moreover, the Equi-Frequency Contours (EFC), i.e. the intersection of the 3D dispersion curves with a horizontal plane, are circular: it means that the wavevector of the elastic wave and the group velocity are antiparallel, for any propagation direction (Fig. 2). As expected, the radius of the EFC clearly decreases as the frequency increases.

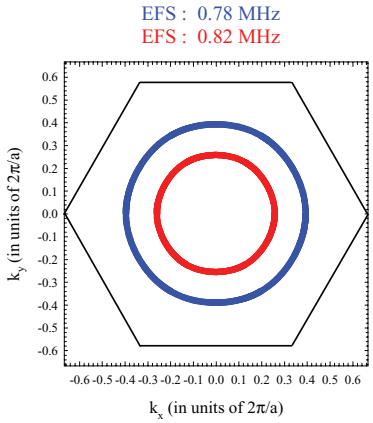

FIG. 2. Equi Frequency Contours of the PC at 780 kHz (thick line) and 820 kHz (thin line).

III. PRISM SHAPED PC

Previous experiments have been performed on a prism shaped PC in an epoxy block.[14] Here, the prism shaped PC is immersed in water, in order to confirm that the longitudinal waves exhibiting negative refraction in the PC can be coupled to the surrounding fluid domain. The experimental set-up is presented on Fig. 3. The prism shaped PC is placed between a Technisonic emitting transducer (1MHz, 0.75″) and a detecting hydrophone. The whole system is immersed in a water tank. The working frequency is 780 kHz which is in the negative refraction frequency range. The emitted pulse is normally incident on the first interface and goes through the PC along the ΓX direction. This wave reaches the second interface with an angle of incidence equal to 60° and then is refracted in water. A hydrophone is used to measure the pressure along a line parallel to the exit surface of the PC, with a 0.4 mm-step. A two dimensional Fourier transform is performed in the measured pulse, allowing the refracted wave amplitude to be plotted as a function of the refraction angle. Fig. 4 presents the variations of the normalized amplitude of the pressure in the fluid along a line 50 mm away from the exit interface of the prism shaped PC, as a function of the refraction angle. Several peaks are observed on the figure; in particular it clearly shows one main peak in the negative part of the angles (-16°), which is consistent with classical Snell-Descartes law. One can notice that the exit angle is much smaller than 60° because the velocity in the PC and the velocity in water are not matched.[14] A second peak located in the positive angle region is due to the positive refraction of another propagating Bloch wave in the PC.[15]

IV. PC FLAT LENS

In this section, in order to check that the negative index PC allows the realization of flat super-lenses able to focus acoustic waves, a flat lens is considered, containing a PC which is 7 cells thick and 65 cells wide. In the PC, the ΓX direction is perpendicular to the interfaces. A point source is placed 3 mm away from the flat lens and an image is observed on the other side of the flat lens. When the indices of the PC and of the surrounding medium are matched, the image of a point source is a point and the distance between the source and its image is equal to twice the flat lens thickness.[6] However, in the studied device, the refraction index of the PC is not matched with the refraction index of water, for immersed applications. In fact, at 786 kHz, which is in the frequency range where negative refraction can occur, the phase velocity is 5676 m/s, which is far from the wave velocity in water (1489 m/s). Therefore, for the study of the focalization phenomena in the external fluid medium, numerical calculations are performed with a fictitious fluid, which index is matched to the PC index. Figure 5 presents the computed pressure field. Because of the impedance mismatch between the PC and the surrounding medium, the pressure amplitude above the lens is far lower than the incident pressure (1/100). Nevertheless, a focusing effect appears clearly. The distance between

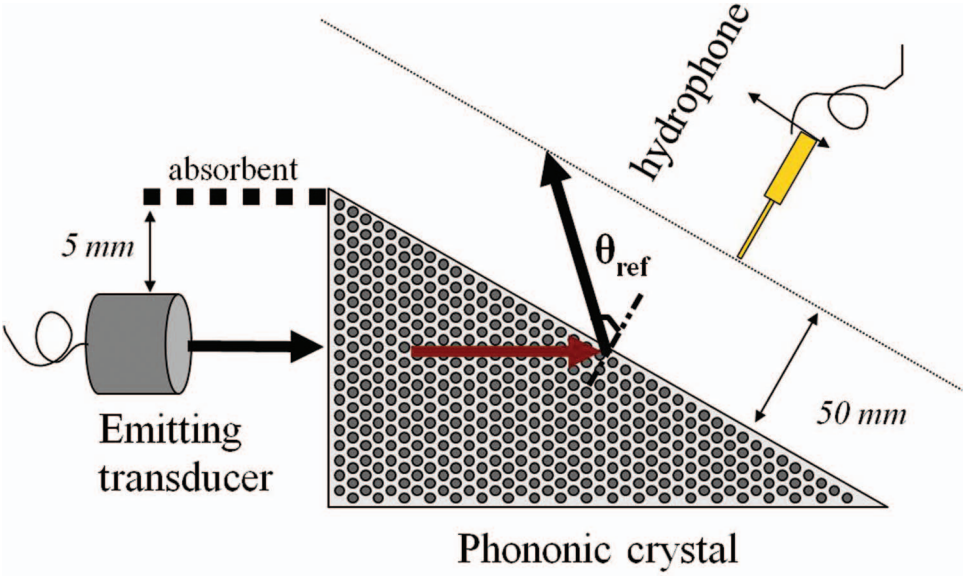

FIG. 3. Schematic description of the experimental set-up in a water tank.

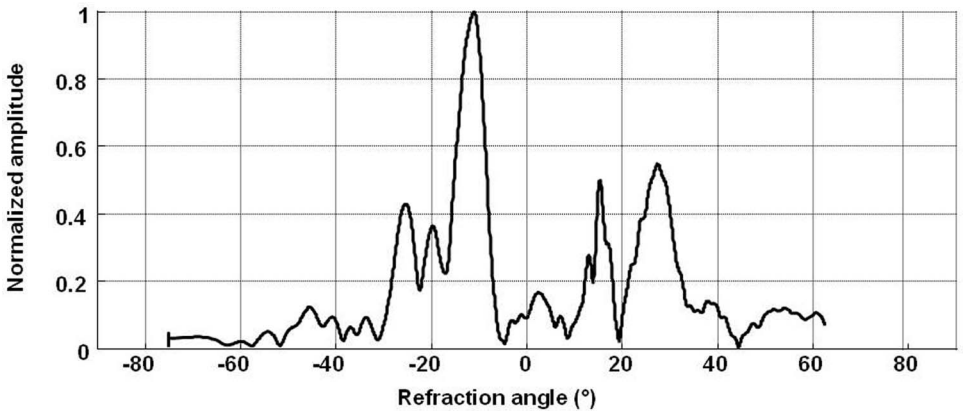

FIG. 4. Amplitude (in arbitrary units) of the measured pressure field in water along a line parallel to the exit surface of the PC, at a distance of 50 mm.

the source and its image is approximately twice the lens thickness, which is consistent with theory.[16] Analysis has been performed on the width and the length of the focal spot, showing that, due to the impedance mismatch between the PC and the surrounding medium, the focal spot is degraded with respect to previous studies on the ideal case.[14]

By looking carefully to the pressure field displayed on Fig. 5, one can notice a second focal point in the area above the flat lens. This second spot takes its origin in the acoustic impedance mistmatch between the PC inside the flat lens and the external fluid medium. As explained on Fig. 6, additional reflections can occur inside the slab that could contribute to the apparition of other images. By simple geometrical considerations, the distance between the two images is equal to twice the lens thickness. In the same way, another spot also appears in the area below the flat lens, but it is not visible in that case (Fig. 6).

Figure 5 clearly shows that some directions are allowed for the construction of the image. Therefore, a double space Fourier Transform is performed on the pressure field above the flat lens, presented on Figure 7. In the (k_x,k_y) wavenumber space, main spots are exhibited: they all are placed on a circle of radius equal to $k_0 = 3316$ m^{-1} the wavenumber in the fluid medium. From Figure 7, it is possible to extract the main directions of propagation. Fig 8 displays the amplitude of the signal

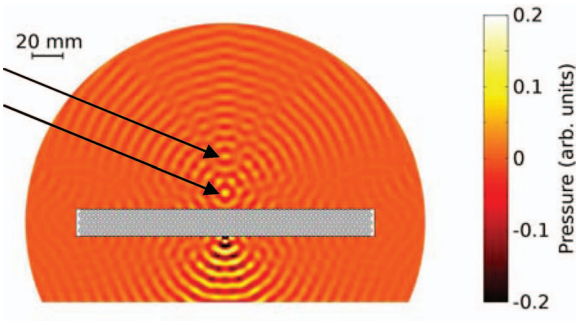

FIG. 5. Simulated pressure field (normalized to a source amplitude of 1 arb. unit) for a PC-made flat lens immersed in a fluid, at 786 kHz. Fluid refractive index is matched to PC index. A point source is located below the lens, 3-mm away from the bottom interface. For clarity, the colorscale is cut to ±0.2 and thus some parts of the field map below the lens are out of colorscale (black/white regions). Losses are not taken into account. The arrows point the focal point and the secondary image.

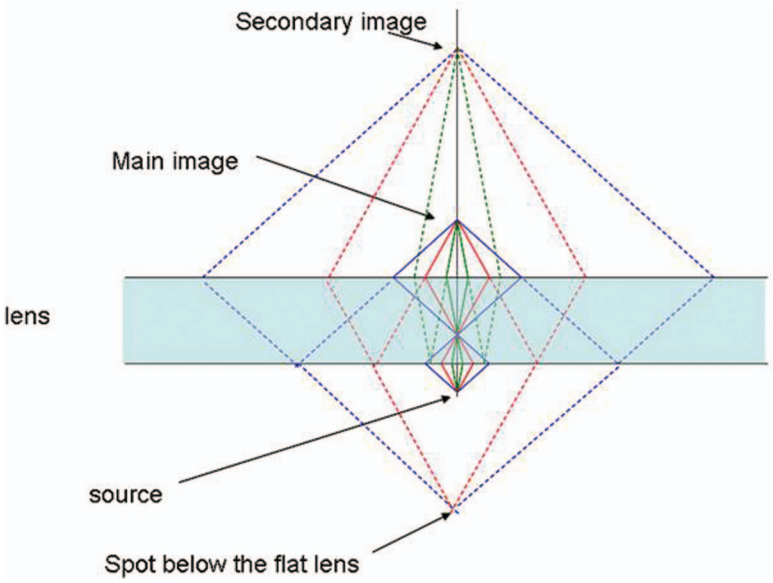

FIG. 6. Geometrical construction of the image of the point source above the flat lens. Due to acoustic impedance mismatch, other spots can be observed.

along the circle of radius k_0. It presents a succession of peaks that are symmetric with respect to the normal to the interface (0°). Waves with either positive or negative angles are excited, which is in accordance with an omnidirectional point source excitation.

V. FLAT LENS WITH EFFECTIVE MEDIUM

In order to understand why some directions are allowed for the construction of the image, the PC constituting the lens is replaced by an effective medium with negative density and negative compressibility producing index matching and impedance mismatch with respect to the external medium. The resulting impedance is equal to one tenth of the external fluid impedance. Lens dimensions, excitation position and frequency are the same as in the case of the flat lens with the PC. The corresponding pressure field is presented on Fig. 9. The similarities between Fig. 5 and Fig. 9 are clear. Several spots are observed in the pressure field: the main spot in the area above the lens corresponds to the image of the point source and is placed approximately at a distance equal to

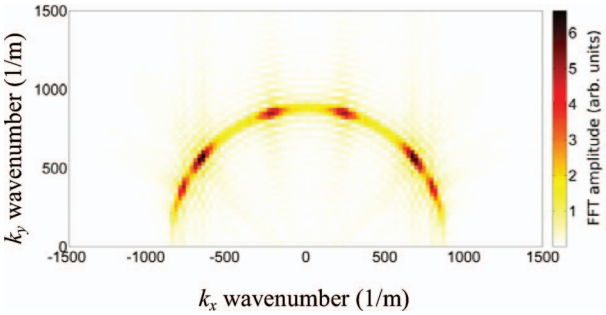

FIG. 7. Double space Fourier Transform on the pressure field of Fig. 5. Main spots are observed that are placed on a circle of radius k_0 (wavenumber in the external fluid medium).

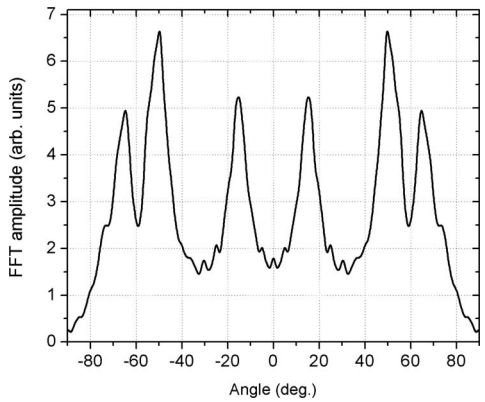

FIG. 8. Amplitude of the signal (Fig. 7) along the circle of radius k_0.

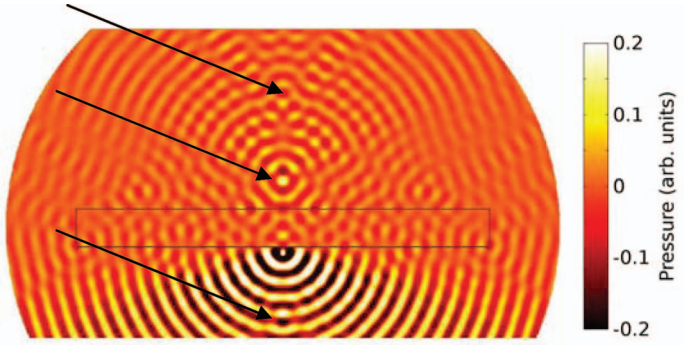

FIG. 9. Simulated pressure field (normalized to a source amplitude of 1 arbit. units) for a flat lens immersed in a fluid, at 786 kHz. The flat lens contains an effective fluid medium, with a negative density and a negative compressibility. Indices between the two media, outside and inside the flat lens are matched. A point source is located below the lens, 3-mm away from the bottom interface. For clarity, the colorscale is cut to ± 0.2 and thus some parts of the field map below the lens are out of colorscale (black/white regions). Losses are not taken into account. The arrows point the focal point and the other images.

twice the lens thickness. Moreover, a second image spot is observed above the first one, and in the area below the flat lens, a small spot is observed, as expected on Fig. 6.

In order to determine the allowed directions in the pressure field, a double space Fourier Transform is once again performed on the pressure field in the region above the flat lens and the corresponding result is presented on Fig. 10. Main spots are observed on the figure, all placed on a circle of radius k_0. The amplitude of the signal along the circle of radius k_0, is presented on Fig. 11. It exhibits a succession of peaks that are symmetric with respect to the normal to the interface (0°). Once again, similarities are observed between the PC-made flat lens and the lens

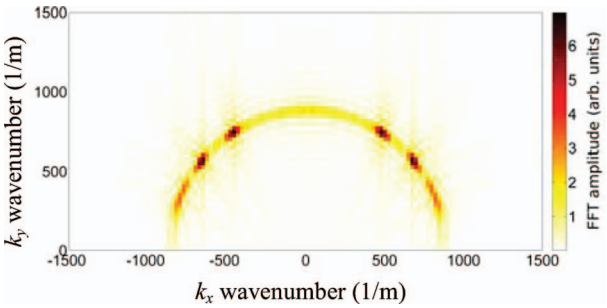

FIG. 10. Double space Fourier Transform on the pressure field of Fig. 9. Main spots are observed that are placed on a circle of radius k_0 (wavenumber in the external fluid medium).

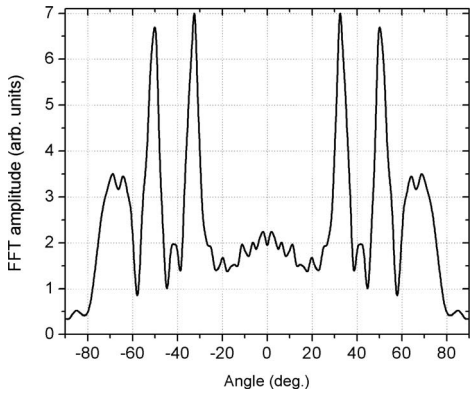

FIG. 11. Amplitude of the signal (Fig. 10) along the circle of radius k_0.

considered as an effective medium (Fig. 8 and 11). The question of the origin of the peaks is raised. As previously noticed, even if the acoustic impedances are not matched, the image is built. But, due to the impedance mismatch between the two media, stationary field in the lens suggests that specific modes are excited. In order to check this point, a modal analysis is performed on the lens alone with the effective properties. Around 786 kHz, which is the frequency of the excitation, two internal resonances of the lens are found (Fig. 12), that are symmetric with respect to the middle of the slab. They correspond to modes ($m = 40$, $n = 3$) and ($m = 28$, $n = 4$) where m and n denote respectively the number of half wavelengths along x and y directions. In the external fluid medium, the wavevector $k_x = m\pi / W$ (where W is the width of the lens) corresponds to an angle of radiation with respect to the normal to the interface $\theta = a \sin(k_x / k_0)$ of $\pm 50.7^\circ$ for the first mode and $\pm 32.8^\circ$ for the second mode. These two directions are exhibited on Fig. 11 and correspond to the main peaks on the figure. Therefore, the wavenumbers associated to internal resonances of the lens contribute to the construction of the image. In order to increase the number of internal resonances of the lens that can participate to the formation of the image, a thicker and larger lens has to be considered because a higher modal density leads to an improved image resolution involving more wavenumbers. A comparison between the PC slab (Fig. 8) and the effective medium (Fig. 11) shows that both cases present peaks approximately at the same position ($\pm 70^\circ$ and $\pm 50.7^\circ$), whereas the peaks at smaller angles nearer the normal to the slab differ between the PC slab and the effective medium. In fact, comparing modes of a flat lens with effective properties and modes of a microstructured material remains difficult and could explain the observed shifts of the peaks.

VI. CONCLUSION

A PC that exhibits negative refraction for longitudinal waves has been presented. Experiments carried out on a prism shaped PC immersed in water allowed to verify its negative index property.

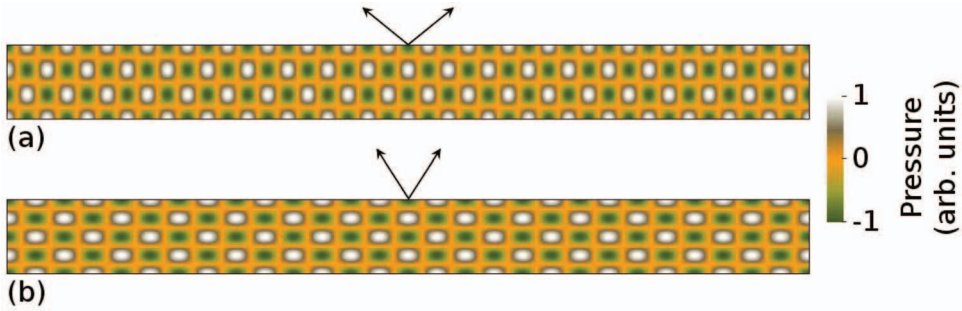

FIG. 12. Lens resonances around excitation frequency, obtained by a modal analysis. (a) mode (40, 3), (b) mode (28,4). Mode (*m*,*n*) denotes mode order for which *m* and *n* are respectively the number of half wavelengths along *x* and *y* directions. The arrows denote the direction of the wavevector of the corresponding mode.

In order to check the focusing capability of the PC, a flat lens has been considered. With the aim of obtaining a high resolution when building images with negative refraction PC, index matching between the medium inside the flat lens and the surrounding medium is necessary.[6] It has been demonstrated that the image of a source can be built even if there is an acoustic impedance mismatch between the two media. In that case, resonant transmissions contribute to the construction of the image. With a larger and thicker lens, resolution can be improved by the increase of the modal density.

ACKNOWLEDGMENT

This work is supported by the Agence Nationale de la Recherche: ANR-08-BLAN-0101-01, SUPREME project.

[1] Xiangdong Zhang and Zhengyou Liu, App. Phys. Lett. **85**, 341 (2004).
[2] Manzhu Ke, Zhengyou Liu, Chunyin Qiu, Wengang Wang, and Jing Shi, Phys. Rev. B **72**, 064306 (2005).
[3] Manzhu Ke, Zhengyou Liu, Zhigang Cheng, Jing Li, Pai Peng, and Jing Shi, Sol. State Comm. **142**, 177 (2007).
[4] Liang-Yu Wu, Lien-Wen Chen, and Rex Ching-Cheng Wang, Physica B **403**, 3599 (2008).
[5] Serkan Alagoz, Olgun Adem Kaya, Baris Baykant Alagoz, App. Acoustics **70**, 1400 (2009).
[6] A. Sukhovich, L. J. Jing, and J. H. Page, Phys. Rev. B **77**, 014301 (2008).
[7] A. Sukhovich, B. Merheb, K. Muralidharan, J. O. Vasseur, Y. Pennec, P. A. Deymier and J. H. Page, Phys. Rev. Lett. **102**, 154301 (2009).
[8] J. B. Pendry, Phys. Rev. Lett. **85**, 3966 (2000).
[9] A-C. Hladky-Hennion, J. Vasseur, B. Dubus, B. Djafari-Rouhani, D. Ekeom, and B. Morvan, J. App. Phys. **104**, 064906 (2008).
[10] Chen-Yu Chiang, and Pi-Gang Luan, J. Phys.: Condens. Matter **22**, 055405 (2010).
[11] B. Bonello, L. Belliard, J. Pierre, J. O. Vasseur, B. Perrin, and O. Boyko, Phys. Rev. B **82**, 104109 (2010).
[12] M. Farhat, S. Guenneau, S. Enoch, A. B. Movchan, and G. G. Petursson, App. Phys. Lett. **96**, 081909 (2010).
[13] J. Pierre, O. Boyko, L. Belliard, J. O. Vasseur, and B. Bonello, App. Phys. Lett. **97**, 121919 (2010).
[14] C. Croënne, D. Manga, B. Morvan, A. Tinel, B. Dubus, J. Vasseur and A.-C. Hladky-Hennion, Phys. Rev. B **83**, 054301, (2011).
[15] C. Croënne, B. Morvan, J. O. Vasseur, B. Dubus, A.-C. Hladky-Hennion, IEEE TUFFC **58**, 178-186 (2011).
[16] V. G. Veselago, Soviet Phys. Uspekhi **10**, 509-514, (1968).